JOURNAL OF VIROLOGY, Apr. 2002, p. 3534–3543 Vol. 76, No. 7
0022-538X/02/$04.00+0 DOI: 10.1128/JVI.76.7.3534–3543.2002

Capsid Protein C of Tick-Borne Encephalitis Virus Tolerates Large Internal Deletions and Is a Favorable Target for Attenuation of Virulence

Regina M. Kofler, Franz X. Heinz, and Christian W. Mandl*

Institute of Virology, University of Vienna, Vienna, Austria

Received 17 October 2001/Accepted 8 January 2002

Deletions ranging in size from 4 to 21 amino acid residues were introduced into the capsid protein of the flavivirus tick-borne encephalitis (TBE) virus. These deletions incrementally affected a hydrophobic domain which is present at the center of all flavivirus capsid protein sequences and part of which may form an amphipathic alpha-helix. In the context of the full-length TBE genome, the deletions did not measurably affect protein expression and up to a deletion length of 16 amino acid residues, corresponding to almost 17% of mature protein C, viable virus was recovered. This virus was strongly attenuated but highly immunogenic in adult mice, revealing capsid protein C as a new and attractive target for the directed attenuation of flaviviruses. Apparently, the larger deletions interfered with the correct assembly of infectious virus particles, and this disturbance of virion assembly is likely to be the molecular basis of attenuation. However, all of the mutants carrying large deletions produced substantial amounts of subviral particles, which as judged from density gradient analyses were identical to recombinant subviral particles as obtained by the expression of the surface proteins prM and E alone. The structural and functional flexibility of protein C revealed in this study and its predicted largely alpha-helical conformation are reminiscent of capsid proteins of other enveloped viruses, such as alphaviruses (N-terminal domain of the capsid protein), retroviruses, and hepadnaviruses and suggest that all of these may belong to a common structural class, which is fundamentally distinct from the classical β-barrel structures of many icosahedral viral capsids. The possibility of attenuating flaviviruses by disturbing virus assembly and favoring the production of noninfectious but highly immunogenic subviral particles opens up a promising new avenue for the development of live flavivirus vaccines.

Members of the genus *Flavivirus*, family *Flaviviridae*, such as yellow fever virus, Japanese encephalitis virus, West Nile virus, the dengue viruses, and tick-borne encephalitis (TBE) virus, cause major human health problems in large areas of the world (4). In spite of a long and successful history of vaccinations against some flavivirus diseases, there is a continuing demand for the development of new flavivirus vaccines. Flaviviruses are positive-stranded RNA viruses. The genome consists of a single approximately 11-kb-long RNA molecule that encodes all of the viral proteins in a single long open reading frame flanked by a rather short 5′ and a somewhat longer 3′ noncoding region (24). For many flaviviruses, including TBE virus, infectious cDNA clones have become available during the past two decades (43). This has made it possible to specifically manipulate the genomes of these viruses. Using this technology, a number of approaches to create attenuated flaviviruses that might be used as live virus vaccines have been pursued, including the construction of chimeric flaviviruses (see reference 2 and references cited therein). Ideally, a live virus vaccine is completely apathogenic but remains highly infectious and replication-competent upon peripheral inoculation and thus efficiently induces a protective immune response. Moreover, the ideal live virus vaccine is incapable of reverting to or evolving into a virulent phenotype. In this communication we present the flavivirus capsid protein C as a new target for the generation of attenuated mutants and provide evidence that deletion mutants of this protein fulfill the above-mentioned criteria to a large degree.

Flaviviruses are small, round, enveloped particles that consist of only three structural proteins (24). Two of these, the small protein M (8 kDa) and the large envelope protein E (54 kDa), are located on the outer surface of the virus particle and are anchored by carboxy-terminal transmembrane domains in the viral membrane. The nucleocapsid contained inside is formed by only a single viral protein C (11 kDa) and the RNA genome. Structural and functional properties of flavivirus particles have been intensively studied during the past several years. The emphasis of most of these studies has been on protein E, which plays a crucial role in the viral life cycle, mediating both viral attachment to the host cell and, after receptor-mediated uptake into endocytotic vesicles has taken place, acid-induced fusion of the viral membrane with the host membrane, thus allowing the release of the nucleocapsid into the cytoplasm of the cell (10). Structural studies on protein E culminated in the elucidation of the atomic structure of the ectodomain of the TBE virus protein E by X-ray diffraction analysis (42). The role played by protein M in the mature virus particle, if any, is probably minor. Its importance derives from the fact that it is formed by a furin-dependent cleavage from a larger precursor protein (prM) that is crucial for assembly of virus particles and protects protein E from premature conformational changes during maturation and release of virus particles (10). Expression of proteins (pr)M and E alone leads to the formation of subviral particles (recombinant subviral particles [RSP]),

* Corresponding author. Mailing address: Institute of Virology, Kinderspitalgasse 15, A-1095 Vienna, Austria. Phone: 43-1-404 90, ext. 79502. Fax: 43-1-404 90-9795. E-mail: christian.mandl@univie.ac.at.

TABLE 1. Primers used for mutagenesis

Orientation	Sequence[a]	Amino acids deleted
Sense	5′-TTTACGCGT-Δ-CAAATGCCAAATGGGCTTGTGT-3′	Q28–V31
Sense	5′-TTTACGCGT-Δ-GGGCTTGTGTTGATGCGCATGA-3′	Q28–N35
Sense	5′-TTTACGCGT-Δ-ATGCGCATGATGGGGATCTTG-3′	Q28–L39
Sense	5′-TTTACGCGT-Δ-GGGATCTTGTGGCATGCCGTA-3′	Q28–M43
Sense	5′-TTTACGCGT-Δ-GCCGTAGCCGGCACCGCGAGAA-3′	Q28–H48
Antisense	5′-AGCGTAAACCGGTGCCAAAC-3′	

[a] Restriction enzyme recognition sequences are underlined; Δ indicates the position of the deletion relative to the wild-type sequence.

which possess many structural and functional properties of infectious virus particles, including the presence of a lipid membrane and the arrangement of the surface proteins in an icosahedral lattice (7, 45). Importantly, RSPs are excellent immunogens capable of inducing a protective immune response that is functionally superior to using protein E in a nonparticulate form (11). Subviral particles which may be identical to RSPs have been observed in variable amounts as a by-product of normal flavivirus replication in cell culture and have been referred to as slowly sedimenting hemagglutinin (44).

Comparatively little is known about the structural and functional properties of protein C. It is a relatively small protein that shares less sequence homology among different flaviviruses species than do the other two structural proteins (31). Consistent with its presumed role in packaging the viral RNA, it is rich in basic amino acid residues. Within the large open reading frame that encodes all of the flavivirus proteins as a single polyprotein precursor, protein C is located at the very amino-terminal end and is thus synthesized first during translation. It is followed by the other two structural proteins, (pr)M and E. The carboxy-terminal region of protein C serves as an internal signal sequence that initiates translocation of protein prM into the lumen of the endoplasmic reticulum (ER). Later during synthesis, this signal sequence, which initially anchors protein C to the ER membrane, is cleaved off by the action of the viral protease NS2B/3, and this cleavage is required to allow the subsequent liberation of the amino terminus of protein prM through the action of host cell signalase (24). Protein C, however, probably remains closely associated with the membrane by virtue of a second hydrophobic element that is present in all flavivirus sequences, approximately in the middle of the primary amino acid sequence (35). This element, termed the internal hydrophobic domain, exhibits features reminiscent of a signal sequence. So far, no high-resolution data on the structure of protein C are available, but electron microscopy studies and the icosahedral organization of the outer viral surface imply that the capsid formed by protein C has icosahedral symmetry.

In this study we constructed mutants of TBE virus that carried deletions in the central region of protein C affecting to various degrees the internal hydrophobic domain, part of which may fold into an alpha-helix that exhibits features of a leucine zipper motif. We observed that as they increased in size the deletions impaired the assembly of infectious virus particles but allowed the formation and secretion of subviral particles. Up to a deletion length of 16 amino acid residues, infectious virus was recovered, and the mutant lacking 16 amino acids proved to be highly attenuated and immunogenic in mice.

MATERIALS AND METHODS

Virus, plasmids, and RSPs. Western subtype TBE virus strain Neudoerfl has been characterized in detail, including the determination of its entire genomic sequence (31, 32), which is available under GenBank accession number U27495. It was used as the wild-type control in all experiments, and all of the described mutants were derived from this strain. Purified virions to be used as controls in gradient centrifugation experiments were prepared from infected chicken embryo (CE) cell culture supernatants as described previously (14). Infectious RNA corresponding to the genome of TBE virus strain Neudoerfl was synthesized in vitro from previously established infectious cDNA clones (30). Plasmid pTNd/c contains a full-length genomic cDNA insert, and RNA transcribed from this plasmid was used as the wild-type control in RNA transfection experiments. Plasmids pTNd/5′ and pTNd/3′ contain cDNAs corresponding to the 5′ one-third and the 3′ two-thirds of the genome, respectively, and can be used to obtain infectious full-length RNA after in vitro ligation. These plasmids were utilized for the construction of specific deletion mutants.

Clone ΔNS5 is a replication-deficient derivative of full-length clone pTNd/c (our unpublished results). ΔNS5 was constructed by deleting the region between two *Bss*HII restriction sites at positions 9880 and 10695 in pTNd/c. This removed the carboxy-terminal 165 amino acid residues of the NS5 protein and essentially the entire variable region of the 3′ noncoding sequence (51).

Purified RSPs used as controls in gradient centrifugation experiments were obtained following previously established procedures by expressing the proteins prM and E from the plasmid SV-PEwt in COS-1 cells (45).

Computer-assisted sequence analysis. Secondary-structure predictions were performed by using the package EMBL PredictProtein (http://www.embl-heidelberg.de/predictprotein/predictprotein.html) and the program COILS (http:/www.ch.embnet.org/software/COILS_form.html) (window size 14) (27, 28). Hydrophobicity calculations based on the algorithm of Kyte and Doolittle (window size 11) (20) and sequence statistics were carried out by using PROTEAN (DNASTAR, Inc.).

Cloning and sequencing procedures. All deletions were introduced into plasmid pTNd/5′ by taking advantage of unique cleavage sites within this plasmid for the restriction enzymes *Mlu*I and *Age*I at positions 208 and 960 of the TBE genomic sequence, respectively. PCR fragments spanning this region and carrying the desired deletion mutations were prepared and substituted for the wild-type sequence by standard procedures. The sequences of the mutagenic sense primers and the wild-type antisense primer that was used for all constructs are listed in Table 1. In order to introduce the deletion mutations into the full-length cDNA clone, the unique cleavage sites for the restriction enzymes *Sal*I, located upstream of the TBE 5′ end (30), and *Sna*BI, at position 1883 in the TBE genome sequence, were utilized to swap fragments from the pTNd/5′-derived mutant plasmid into plasmid pTNd/c. Plasmids were amplified in *Escherichia coli* strain HB 101, and small- and large-scale plasmid preparations were made by using Qiagen purification systems. New constructs were checked by sequence analysis, including at least the region synthesized by PCR and the vicinity of the utilized insertion sites.

Sequencing was performed using an automated DNA sequencing system (ABI). The genome sequence coding for protein C was checked for all stock virus suspensions prior to biological characterizations by reverse transcription-PCR and direct sequence analysis as described previously (51).

RNA transcription and transfection and stock virus preparations. RNA was transcribed from full-length cDNA clones or in vitro-ligated templates by using T7 polymerase (Ambion) and transfected into BHK-21 cells by electroporation under the conditions described previously (30). Supernatants that were found to contain infectious virus were used to infect litters of suckling mice (0 or 1 day old) for the preparation of high-titer virus stocks as described in detail elsewhere (30).

Cell cultures. BHK-21 cells, porcine kidney (PS) cells, and primary CE cells were grown under standard conditions (16, 30). Infectivity values of virus stocks were determined by plaque titer determinations on PS cells (16) and confirmed by endpoint dilution infection experiments on BHK-21 and CE cells. Growth curves on CE cells were performed as described in detail elsewhere (30). Briefly, cells were infected at a multiplicity of infection (MOI) of approximately 1, and virus released from the cells within 1-h periods was collected from the supernatant at several times postinfection and quantified by standard plaque assays.

Detection and quantification of protein E expression. Expression of protein E in BHK-21 cells was visualized 48 h posttransfection by immunofluorescence staining after fixation of cells with acetone-methanol (1:1) using a polyclonal rabbit anti-protein E serum and fluorescein isothiocyanate-conjugated anti-rabbit antibody. Protein E released into the supernatant of cell cultures was detected by a four-layer enzyme-linked immunosorbent assay (ELISA) (15). For passaging experiments, supernatants were cleared from cell debris and insoluble material by low-speed centrifugation and the E protein content was measured by sodium dodecyl sulfate (SDS)-ELISA (12). Then, aliquots containing equal amounts of protein E (20 ng) were transferred to new BHK-21 cells and protein E expression in these cells was determined as before.

For a quantitative analysis of protein E expression, BHK-21 cells were counted after RNA transfections by using a Casy 1 TT cell counter (Schärfe Systems) and equal numbers of vital cells were seeded into culture flasks (Nunc). Cells were allowed to grow for 12 h with 5% fetal calf serum, after which the fetal calf serum concentration was reduced to 1%. At defined time points (24 and 30 h posttransfection), supernatants and cells were harvested separately. Aliquots of supernatants were used for measurement of protein E content using an SDS-ELISA (12). Cells were detached from the culture bottles by trypsin incubation and scraping and counted as before, and aliquots of 10^6 cells were suspended in lysis buffer (TAN buffer, consisting of 0.05 M triethanolamine [pH 8.0] and 0.1 M NaCl, plus 1% Triton X-100) and incubated for 15 min at 4°C. Lysates were cleared by low-speed centrifugation, and the protein E content was quantified by SDS-ELISA (12). To correct for the variability caused by different transfection efficiencies, virus spread, or total cell numbers, the number of protein E-producing cells was calculated for each sample at the corresponding time point. For this purpose, aliquots of the cell preparations were stained with a monoclonal antibody directed against protein E (B2) and specifically labeled cells were counted in a FACSCalibur flow cytometer (Becton Dickinson).

Particle analysis. BHK-21 cells were transfected by electroporation with in vitro-synthesized mutant RNAs and mixed with untransfected cells to allow for secondary infections. Forty-eight hours postinfection, supernatants were harvested and viral and subviral particles were pelleted by ultracentrifugation (Ti 45 rotor [Beckman], 44,000 rpm, 2 h, 4°C). The resuspended pellets were analyzed by rate zonal gradient centrifugation. Discontinuous sucrose gradients (10, 35, and 50% sucrose in TAN buffer containing 0.1% bovine serum albumin) were utilized to achieve an optimal separation of virions from subviral particles (SW 55 rotor [Beckman], 44,000 rpm, 4 h, 4°C). Gradients were fractionated using an ISCO 640 gradient fractionator, and protein E content of individual fractions was determined by SDS-ELISA (12). Buoyant densities were determined by equilibrium centrifugation on continuous sucrose gradients (20 to 50%) essentially as described before (45). The sucrose density of the particle-containing fractions was determined with an Abbe refractometer (Atago) correcting for temperature using standard tables (ISCO).

Animal model. The characterization of mutant viruses in the mouse model was performed as in previous studies (29, 33, 34). Briefly, groups of 10 5-week-old (body weight, approximately 20 g) outbred Swiss albino mice were inoculated subcutaneously, and survival was recorded for 28 days. Then the mice were bled, and seroconversion was detected by a TBE antibody ELISA (13). For the determination of the 50% lethal dose (LD_{50}) and the 50% infective dose (ID_{50}), groups of 10 mice were inoculated with sequential 10-fold dilutions of virus ranging from 1 to 10^6 PFU. The calculation of LD_{50} and ID_{50} values was performed by the method of Reed and Muench (41). For ID_{50} calculations, the number of infected mice was taken to be the total of mice killed plus surviving mice with detectable seroconversion. Surviving mice without detectable serum antibody were scored as uninfected. To test whether seroconverted mice had developed a protective immunity, mice were challenged with the highly virulent TBE virus strain Hypr (50) in a high dose (>100 LD_{50}) that typically kills 100% of nonimmunized mice.

RESULTS

Computer-assisted analysis of the TBE virus capsid sequence. Protein C of TBE virus is a 116-residue-long highly basic protein (calculated isoelectric point 12.5) containing a total of 11 arginine and 12 lysine residues. Secondary-structure prediction using the program PredictProtein (EMBL) revealed two particularly noteworthy features of this sequence, which are illustrated in Fig. 1. First, in spite of the high overall proportion of charged amino acid residues, there are two distinct hydrophobic domains. Secondly, the secondary-structure conformation of protein C is predicted to be largely alpha-helical. The employed algorithm strongly predicted the formation of four helices that would take up most of the carboxy-terminal two-thirds of the protein. Helix IV corresponds to the hydrophobic carboxy-terminal end of protein C, which is known to act as an internal signal sequence for the translocation of the subsequent protein prM into the lumen of the ER and is removed from mature protein C by the action of the viral protease NS2B/3 (24). Helix I is part of the central hydrophobic domain, which extends approximately from residues 34 to 51 (exact boundaries vary depending on the algorithm and parameter settings used). Part of this region was previously proposed to anchor mature protein C into the viral membrane (35). Close inspection of the sequence revealed that both helix I and helix III are amphipathic and exhibit a periodical heptad organization of leucine residues (Fig. 1). These features are reminiscent of leucine zipper motifs which are known to have a high propensity to form coiled-coil interactions (27, 28). Coiled-coil interactions are in fact predicted in the case of helix III by the COILS algorithm, whereas helix I, which consists of only two full heptad repeats, is too short to be submitted to this analysis.

Generation of deletion mutants. We wanted to study the effects of mutations in protein C on the expression, particle formation, viability, and virulence of TBE virus. We anticipated that major changes within the amino- and the carboxy-terminal regions of protein C would be deleterious for the virus. Therefore, we chose the central domain, in particular the hydrophobic domain containing helix I, as a target for our analysis. A set of deletion mutations of increasing sizes (removing 4, 8, 12, 16, or 21 amino acid residues) was engineered into the infectious cDNA clone of TBE virus strain Neudoerfl. As shown in Fig. 1, these deletions start shortly before the central hydrophobic domain and, with increasing size, remove incremental parts of this domain but leave the flanking positively charged hydrophilic domain largely unaffected. The largest deletion removes most of helix I including histidine 48. The designations of the resultant mutants as listed in Fig. 1 refer to the locations of the deletions within protein C [e.g., mutant C(Δ28–31) lacks the four amino acid residues 28 through 31 of protein C].

Viability of deletion mutants in BHK-21 cells. The initial step of our characterization of the capsid deletion mutants was to assess their competence for protein expression in BHK-21 cell culture. Since protein expression depends on both translation and replication of the viral genome, an inability to detect protein E in this experiment would suggest that one or both of these functions were significantly impaired by the deletions in protein C. RNAs transcribed from the five mutated and the parental wild-type cDNA clones were transfected into BHK-21 cells and assayed for protein E expression 48 h postinfection. A replication-deficient mutant RNA (termed ΔNS5) was also included in the experiment. As can be seen in Fig. 2a to g, the wild type and all of the mutants yielded positive immunofluo-

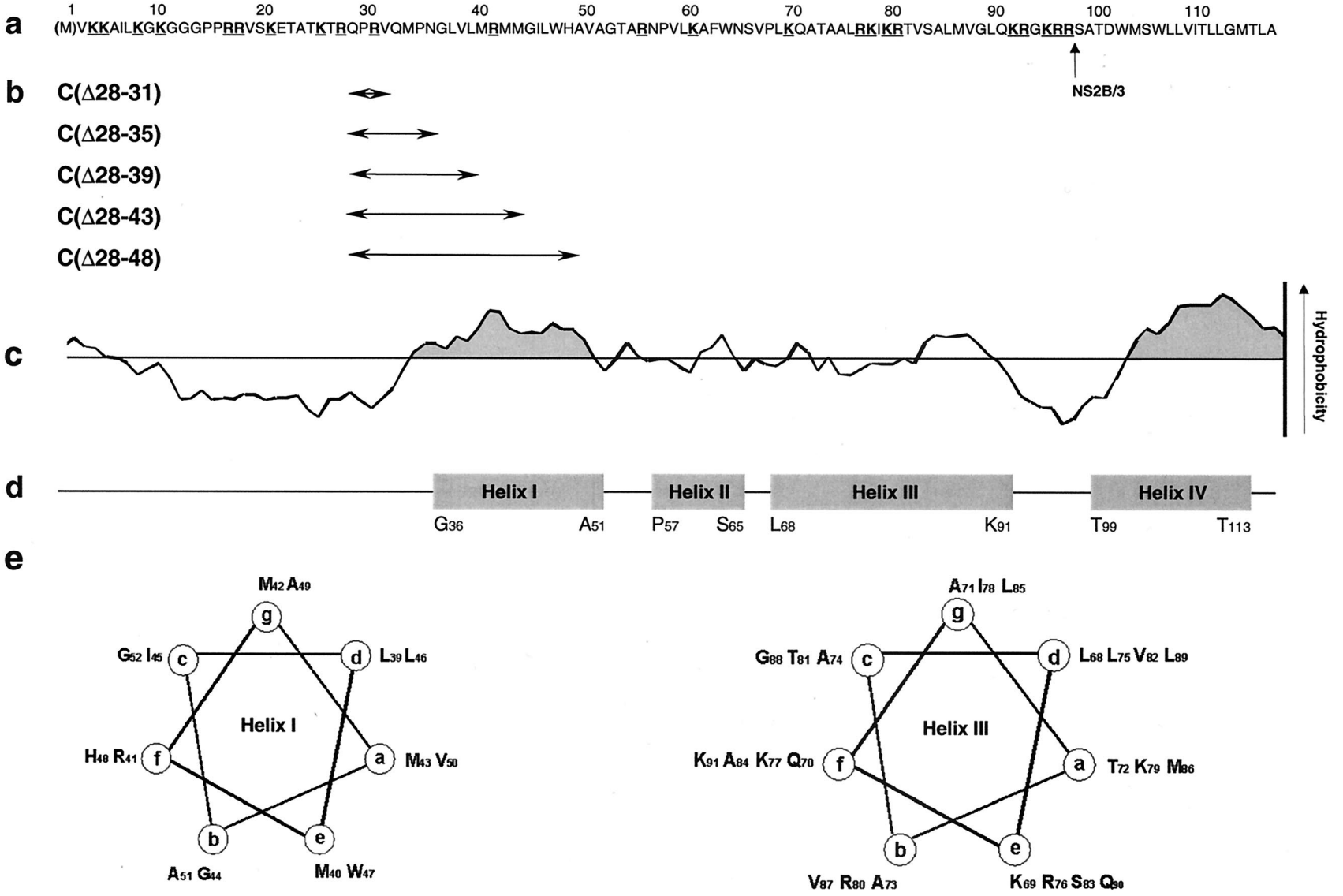

FIG. 1. Characteristics of the TBE virus protein C wild-type and mutant amino acid sequences. (a) Sequence of the wild-type primary translation product, from which the amino-terminal methionine (shown in parentheses) and the carboxy-terminal 20 residues (presumed NS2B/3 cleavage site indicated by an arrow) are removed to yield mature protein C. Positively charged residues are underlined and bold. (b) Locations of the introduced deletion mutations (arrows) together with the designations of the corresponding mutants. The numbers in the names of the mutants indicate which residues were deleted. (c) Hydrophobicity plot calculated using the Kyte-Doolittle algorithm (window size 11) (20). The positions of two extended hydrophobic domains located in the center and at the carboxy terminus of the primary sequence are emphasized by grey shading. (d) Secondary-structure prediction revealing four predicted alpha-helical domains. The positions of the potential helices are indicated by shaded boxes and numbered consecutively by roman numerals. The first and last residue of each predicted helix are listed below the box. (e) Helical wheel representations of two sequence elements exhibiting features of leucine zipper motifs.

rescence staining and protein E was detected by ELISA in the supernatants, too. In contrast, the ΔNS5 control was negative in both tests. These results indicated that the capsid deletion mutants were competent for protein expression in BHK-21 cells and also released protein E into the supernatants. To investigate whether the released material contained infectious particles, aliquots containing 20 ng of protein E were transferred to new BHK-21 cells. These cell cultures were tested for protein E expression as before, and the results are shown in Fig. 2h to n. Clearly, all of the capsid deletion mutants except for the one carrying the largest deletion, C(Δ28–48), were transmitted to new BHK-21 cells. This result was confirmed in a number of independent experiments, in which mutant C(Δ28–48) could never be introduced into new BHK-21 cells, even when supernatants containing up to 10 times more protein E were used (data not shown). While expression and particle formation are analyzed in more detail below, the main conclusion at this point is that TBE virus is capable of assembling infectious particles in spite of deletions in its capsid protein removing up to 16 amino acid residues, i.e., almost 17% of the length of mature protein C.

Quantification of protein E expression and export. After it was established that the capsid deletion mutants were competent for protein expression and release of protein E from cells, we wanted to determine and compare the efficiencies of these processes. We chose the two mutants with the largest deletions, C(Δ28–43) and C(Δ28–48), for this quantitative analysis and included wild-type and ΔNS5 RNAs as positive and negative controls, respectively. BHK-21 cells were transfected as before, and the amounts of protein E present inside the cells and released into the supernatants were determined at two time points (24 and 30 h posttransfection). Then, the sum of intracellular and extracellular protein E was calculated and this value was normalized for the number of protein-E-producing cells. The results of this analysis, shown in Fig. 3a, demonstrated that mutants and wild-type virus produced approximately equal quantities of protein E per cell at both time points. The amount of protein E translated from the control RNA ΔNS5 remained below the detection limit. Clearly the large deletions in protein C did not measurably diminish protein expression, and it can therefore be concluded that they did not impair RNA replication or translation.

The availability of quantitative data on the amount of intracellular and extracellular protein E obtained in this experiment was then used to evaluate the efficiency of protein E release from BHK-21 cells. Efficient release of protein E depends on its proper processing and assembly into viral or subviral particles. The results shown in Fig. 3b indicated that the amounts of protein E released were diminished for both mutants, and this effect was more pronounced at the earlier time point. The reduction and delay of protein E release in the case of the capsid deletion mutants suggest an influence of these mutations on particle formation, and this is investigated in more detail below.

Formation of viral and subviral particles. Flavivirus structural proteins can, in principle, assemble into two different forms of particles: (i) nucleocapsid-containing virions with a diameter of 50 nm and a buoyant density of 1.19 g/cm^3 and (ii) capsidless, noninfectious subviral particles with a diameter of only approximately 30 nm and a buoyant density of only 1.14 g/cm^3 (45). Rate zonal centrifugation using a discontinuous sucrose gradient yields a clear separation through the accumulation of subviral and viral particles at the 35 and 50% sucrose boundaries, respectively (Fig. 4). The analysis of particles released from BHK-21 cells transfected with the mutant RNAs as shown in Fig. 4 indicated that mutants carrying only small deletions exhibited peaks corresponding to both viral and subviral particles. With increasing deletion sizes, however, larger proportions of subviral particles and decreasing amounts of viral particles were detected in this type of analysis. To better define the physical forms of these particles, similar separations were performed on continuous sucrose gradients and the particle-containing fractions were further analyzed by equilibrium sucrose density centrifugation. This analysis yielded a buoyant density of 1.14 g/cm^3 in the cases of the subviral particle fractions of all of the mutants, strongly suggesting a structural similarity to the RSP control. The buoyant density of the virion fraction of mutant C(Δ28–31) was found to be 1.19 g/cm^3, as was that of the wild-type virus control. In the cases of the mutants carrying larger deletions, C(Δ28–35), C(Δ28–39), C(Δ28–43), and C(Δ28–48), particles that sedimented with velocities between those of the control RSPs and those of the wild-type virus were found (data not shown). Due to the physical instability of these particles, it was not possible to determine their buoyant densities. We assumed that these populations contained forms of virions that assembled incorrectly due to the deletions in protein C.

Growth properties of the mutants. In order to obtain uniform and high-titered virus stocks for all subsequent biological characterizations, mutant viruses C(Δ28–35), C(Δ28–39), and C(Δ28–43) were passaged twice in suckling mouse brains and brain suspensions were prepared from the second round of infection. This yielded stock virus suspensions with infectivity titers that were only approximately 10-fold less than that of a similarly prepared wild-type virus suspension (Table 2). Genome sequence analysis of the protein C-coding region confirmed the presence of the engineered deletion mutations in these virus stocks but did not reveal any additional mutations that might have emerged during the mouse passages.

To characterize the in vitro growth properties of the mutant viruses in more detail, we determined their plaque morphology on PS cells and prepared single-step growth curves on CE cells. Plaques were found to be clear but significantly smaller than those formed by wild-type virus. The information included in Table 2 illustrates that mutants with larger deletions formed even smaller plaques than those with smaller deletions.

To quantitatively compare the production levels of infectious virus particles by mutant and wild-type viruses, single-round growth curves as shown in Fig. 5 were prepared. All of the mutants were found to release significantly fewer infectious particles than did the wild-type virus. The release was especially delayed for the two larger-deletion mutants, C(Δ28–39) and C(Δ28–43), although all three mutants ultimately reached similar maximum values of approximately 10^3 PFU/ml/h.

Virulence properties. Finally, the effects of deletions in the capsid protein were tested in vivo by using an established adult mouse model (33). In this system, infectivity and neuroinvasiveness are determined after peripheral inoculation of virus. Whereas virulent TBE virus induces fatal encephalitis in a large percentage of inoculated mice (neuroinvasiveness), at-

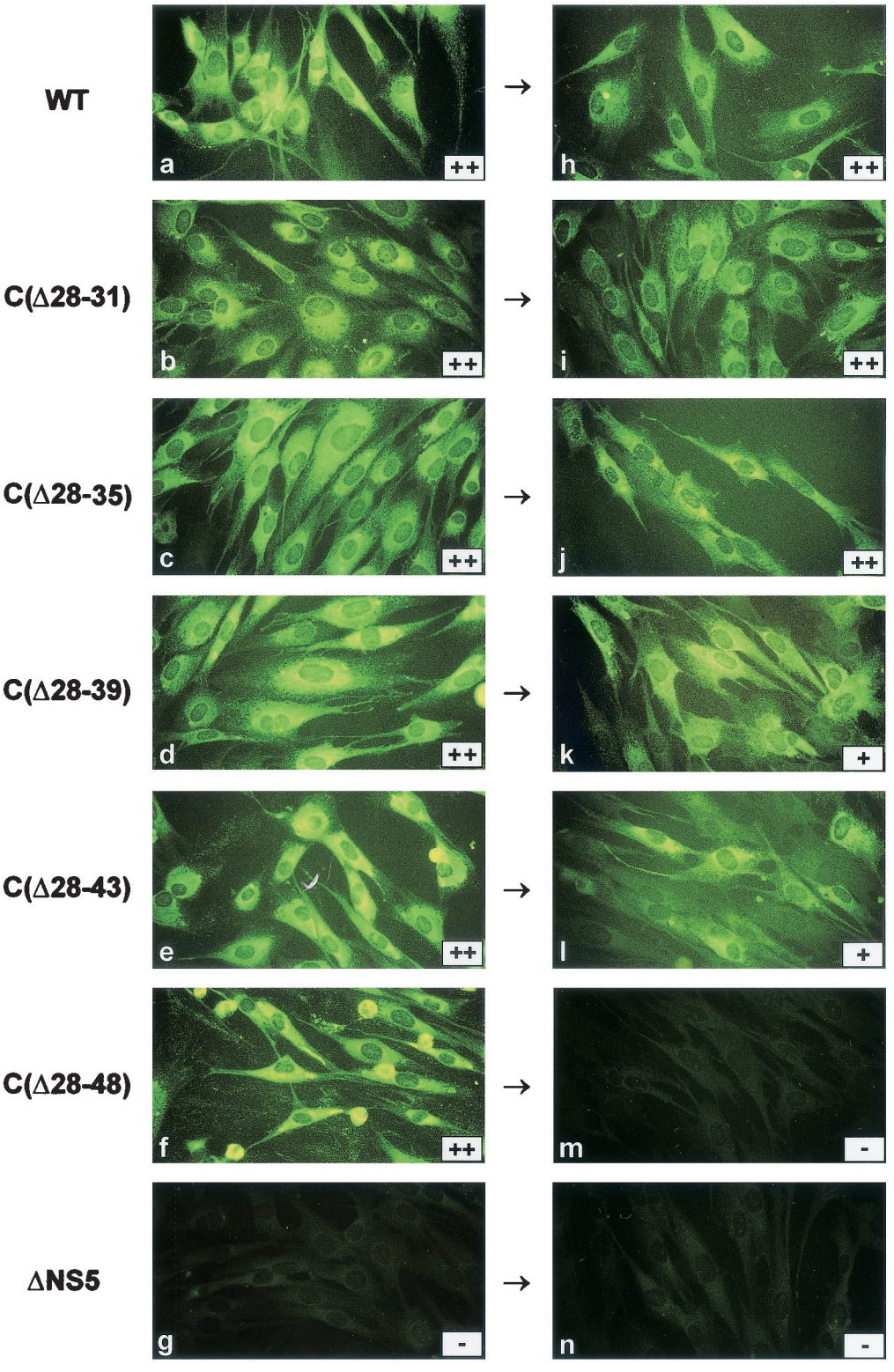

FIG. 2. Expression of protein E and cell culture passage. (a to g) Wild-type (WT) and mutant RNAs (as indicated) were synthesized in vitro and transfected into BHK-21 cells. Expression of protein E was tested 48 h posttransfection by immunofluorescence, and protein E released into the supernatants was detected using a four-layer ELISA. Results of ELISA are given in the inserts as follows: −, optical density (OD) < 0.1; +, OD = 0.1 to 1.0; ++, OD > 1.0. (h to n) Supernatants were passaged onto new BHK-21 cell cultures as symbolized by the arrows, and the expression of protein E was determined 48 h postinoculation by immunofluorescence and ELISA as before.

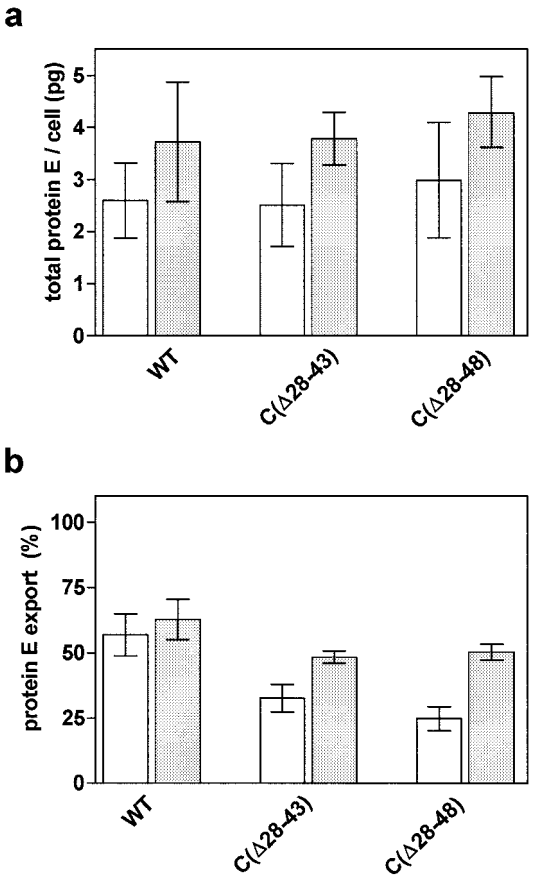

FIG. 3. Quantitative analysis of total protein E expression and export. BHK-21 cells were transfected with in vitro-synthesized wild-type (WT) and mutant RNAs as indicated. The amount of protein E expressed per cell (a) and the percentage of protein E released from the cell into the cell culture supernatant (b) were determined at 24 h (open bars) and 30 h (shaded bars) posttransfection. Results shown are mean values of three experiments (± standard errors of the means).

tenuated mutants do not cause disease but replicate and induce a specific antibody response (infectivity). Using various inoculation doses allows the determination of LD_{50} as a quantitative parameter of neuroinvasiveness and that of ID_{50} as a quantitative parameter of infectivity. With regard to the development of a safe and efficient vaccine the goal is to get a mutant that shows a large LD_{50}/ID_{50} ratio (attenuation index).

Preliminary tests using only one or two different inoculation doses suggested that the mutant carrying the smallest deletion, C(Δ28–31), exhibited properties similar to those of the wild-type virus, whereas the mutants carrying larger deletions appeared to have reduced neuroinvasiveness (data not shown). Assuming that alterations in virulence are more likely to be pronounced with a larger deletion size, we decided to analyze in detail the mutant with the largest deletion that was still viable, i.e., mutant C(Δ28–43). The LD_{50}s and ID_{50}s derived from this experiment are listed in Table 2 and compared to the previously determined values of wild-type TBE virus (33). It turned out that mutant C(Δ28–43) was highly attenuated. Not a single mouse at any inoculation dose developed signs of disease. This meant that the LD_{50} exceeded $10^{6.5}$, and thus, the attenuation index of this mutant was 3.9 or higher. To test whether this mutant was capable of inducing a protective immunity, mice were challenged with the virulent TBE virus strain Hypr. All of the mice that had been infected and had seroconverted were completely protected against disease. Consequently, the 50% protective dose was equal to the ID_{50}, i.e., $10^{2.6}$.

DISCUSSION

Closed-shelled virus particles with icosahedral symmetry are often composed of typical wedge-like building blocks that are formed by characteristic eight-stranded antiparallel β-barrel structures, also known as jelly-roll beta-barrels (9). However, icosahedral capsids can apparently also be formed by another kind of capsid protein that is characterized by a large proportion of alpha-helical structure. Hepadnavirus and retrovirus capsid proteins are prominent representatives of this type (38, 52). In both of these cases the capsid proteins dimerize by the association of two amphipathic alpha-helical hairpins that form so-called four-helix bundles (55). Bacteriophage ϕ6 is another example of a spherical shell formed by a largely alpha-helical protein (3). The capsid protein of alphaviruses consists of two distinct domains. The structure of the carboxy-terminal autoprotease domain has been solved by X-ray crystallography, but the amino-terminal domain appeared unstructured in these analyses and its exact structure remained unsolved (5, 6). This domain appears to be structurally and functionally flexible (8), and a recent study has revealed the presence of a conserved amphipathic helix containing a leucine zipper motif that has been proposed to function in core assembly through specific coiled-coil interactions (40). It is possible that the amino-terminal domain of alphavirus capsid proteins may belong to the same class of capsid proteins to which hepadnavirus and retrovirus capsids belong. Our analysis now suggests that the flavivirus capsid protein may also belong to the same structural category: both the predicted high content of alpha-helical structure and the potential to engage in coiled-coil interactions as well as the considerable structural and functional flexibility revealed in this study resemble results obtained for alphaviruses (8). The recent finding that the alphavirus surface glycoprotein E1 shares a very similar overall fold with the flavivirus envelope protein E strongly implies that these two virus families are structurally closely related (23). It is tempting to speculate that their capsid proteins may also have similar structures and that they both may be members of a structural category possibly common among capsids of enveloped viruses.

There are, however, obvious and major differences between the alphavirus and the flavivirus capsid proteins and their role in virus assembly. Flavivirus capsid proteins are smaller and apparently lack the region corresponding to the alphavirus carboxy-terminal autoprotease domain. Instead, the carboxy terminus of the flavivirus protein C is formed by the action of the viral protease NS2B/3 (24). In the absence of capsid protein, the flaviviral surface proteins (pr)M and E efficiently assemble into smaller icosahedral (T=1) subviral particles (see references 7 and 45 and references cited therein), a process that has not been identified for alphaviruses. There is a specific interaction between residues of the cytoplasmic domain of the alphavirus E2 protein and the capsid protein which is important for virus assembly (22, 39, 46–49, 54). In contrast, the

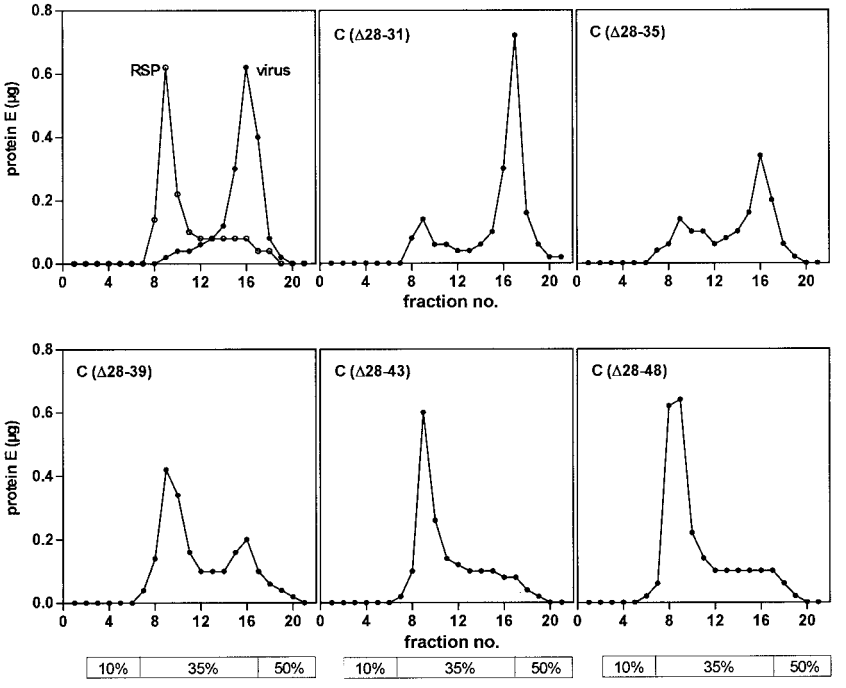

FIG. 4. Particle analysis by rate zonal centrifugation. Control preparations of wild-type virus and RSPs as well as particles pelleted from BHK-21 cell supernatants after transfection with the indicated mutant RNA were fractionated on discontinuous sucrose gradients. The 10, 35, and 50% zones are indicated below the graphs. The protein E content of each fraction was determined by a quantitative SDS-ELISA.

cytoplasmic domains of the flaviviral surface proteins are extremely short and it is unknown how they might interact with the capsid. One possibility may be that interactions occur inside the viral membrane between a transmembrane domain of a surface protein and a domain of protein C that is inserted into the membrane. Markoff et al. have demonstrated that an internal hydrophobic domain of dengue virus type 4 protein C shares properties of an internal signal sequence and this domain inserts into a membrane in a hairpin conformation (35). These authors recognized the presence of similar internal hydrophobic sequences in all flavivirus capsid sequences and suggested a general role of this domain in anchoring protein C to the membrane. Similar results have been reported for hepatitis C virus, another member of the *Flaviviridae* (25). Our results are compatible with the hypothesis that this hydrophobic domain is involved in interactions between the capsid and viral surface proteins: the removal of incremental parts of the internal hydrophobic domain of the TBE virus capsid protein impaired the assembly of infectious virus particles but still allowed or even favored the assembly of capsidless subviral particles. The quantity of subviral particles formed during infections with wild-type TBE virus appears to depend on a number of factors, such as the MOI and the particular host cell type utilized (our unpublished observation). This makes it difficult to exactly determine to what extent the deletions shifted assembly towards the synthesis of subviral particles. The observation that efficient generation and export of subviral particles could occur even with large deletions suggests, however, that these mutations predominantly impaired the assembly or

TABLE 2. Biological properties of deletion mutants

Virus	Infectivity titer of virus stock (log PFU/ml)	Plaque size (mm)	LD_{50} (log PFU)	ID_{50} (log PFU)	LD_{50}/ID_{50} attenuation index (log)
Wild type	8.4	2–3	0.9	−0.2	1.1
C(Δ28–35)	7.7	1–2			
C(Δ28–39)	7.7	≤1			
C(Δ28–43)	7.5	<1	≥6.5	2.6	≥3.9

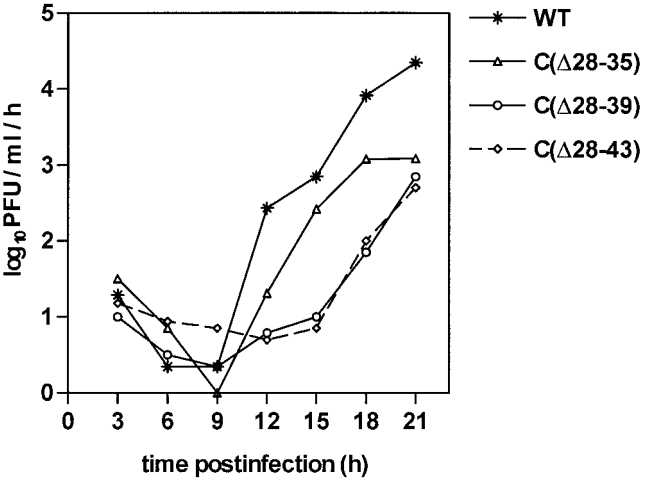

FIG. 5. Growth curve analysis of wild-type and mutant TBE viruses. CE cells were infected at a MOI of 1, and the amounts of infectious particles released into the supernatants during 1-h time periods were quantified at various time points postinfection.

stability of viral particles but left other functions, such as the proteolytic processing of the polyprotein, largely unaffected.

In the case of hepatitis C virus, numerous functional activities have been associated with its core protein (36). This may also be the case for TBE virus and other flaviviral capsid proteins. In the Kunjin virus system two domains (residues 3 to 32 and 84 to 107) that are rich in positively charged amino acid residues have been shown to be important for packaging the viral genomic RNA (17). Also in the Kunjin system, it has been demonstrated that the coding region of the first 20 amino acid residues is essential for virus replication (18), and this was recently correlated with the presence of a cyclization sequence in this region (19). In contrast, only the first two amino acid residues were required for efficient translation (18, 19). The role of the carboxy-terminal hydrophobic domain as an internal signal sequence and its removal from mature protein C by the action of the viral protease NS2B/3 have been studied by various researchers (1, 26, 53). Here we tested the functional importance of the central hydrophobic and probably helical domain (helix I) by deleting residues between positions 28 and 48. Deletions within this domain did not significantly impair translation or replication as shown by an efficient protein expression of the deletion mutants. The finding that mutant C(Δ28–43) still produced infectious virus particles also rules out an essential role of this domain for specific RNA packaging. Helix I, however, probably plays a role in virus assembly. The role of helix I may be an intramembraneous interaction with a viral surface protein as discussed above, and/or it may participate in coiled-coil-type interactions of protein C oligomers. This notion is supported by the finding that very similar helical structures are predicted at the corresponding positions of other flavivirus capsid sequences (our unpublished observation). It is likely, however, that helix III, which is twice as long and also contains charged amino acids at positions known to potentially stabilize coiled coils (27), may have a more prominent role in intermolecular interactions of protein C, making helix III an attractive target for future mutagenesis studies.

The most dramatic difference among the mutants tested in this study was observed between mutants C(Δ28–43) and C(Δ28–48). Whereas the former still grew to considerable titers, the latter did not produce any detectable infectious particles in cell culture. In mutant C(Δ28–43), helix I was severely truncated but may still have maintained some functionality. In mutant C(Δ28–48), however, this structure was almost completely removed and also residue His 48, which was previously proposed to be functionally relevant (35), was deleted in this mutant. In addition, it should be noted that the residues still present in mutant C(Δ28–43) but deleted in mutant C(Δ28–48) included the sequence motif M-X-I, which in the case of the alphavirus Semliki Forest virus has been shown to be essential for the formation of intracellular nucleocapsids (47).

Another central aspect of this study relates to the identification of protein C as a new and promising target for the development of live flavivirus vaccines. New vaccines will be needed to meet the various challenges imposed by problems such as the complex pathogenesis of dengue hemorrhagic fever, the socioeconomic situation of third-world countries where flaviviral diseases are most common, or the introduction of flaviviruses into new populations, such as the recent emergence of West Nile virus in North America (21). Although attenuation of flaviviruses has been achieved by numerous approaches including the specific introduction of mutations in structural and nonstructural proteins and the terminal noncoding regions (24, 37), the potential to generate viable mutants carrying deletions in the capsid protein and to achieve significant attenuation by this method had not been recognized until now. Moreover, our data indicated that this attenuation principle has a number of important advantages over other approaches. Unlike most of the mutations that have been introduced into nonstructural proteins or noncoding regions, this attenuation apparently does not rely on diminished translation or replication but maintains a high level of protein expression. This should be beneficial for achieving an efficient and protective immune response. Moreover, all of the known major antigenic targets required for the development of a protective immune response, in particular glycoprotein E, which contains important neutralizing epitopes, are fully intact in these constructs. This should mean a major advantage over approaches that achieve attenuation through various protein E mutations (29, 34, 37). Our data suggest that the attenuation achieved by deletions within the central hydrophobic domain (helix I) of the capsid protein is mainly based on the disturbance of the assembly of infectious virus particles, while still allowing subviral particles to be formed. These subviral particles, however, are noninfectious and known to be excellent immunogens (11). A general advantage of deletion mutations compared to point mutations resides in the practical impossibility of reversion to a wild-type sequence. Although second-site mutations that may increase the virulence cannot be excluded even in the case of deletions, it is highly unlikely that these mutations could restore a fully wild-type phenotype. Finally, the data obtained from our mouse experiments demonstrate the excellent safety and immunogenicity of mutant C(Δ28–43). Among all of the attenuating mutations tested in the TBE virus system so far, this is the first single-mutation mutant that did not cause disease in mice up to the very high peripheral inoculation dose of 10^6 PFU.

The mutants described in this study have opened new avenues for the investigation of structural and functional properties of the flavivirus capsid protein C and at the same time represent a promising starting point for the development of live flavivirus vaccines.

ACKNOWLEDGMENTS

We gratefully acknowledge the excellent technical assistance of Jutta Hutecek, Silvia Röhnke, and Melby Wilfinger, and we thank Steven L. Allison for many helpful discussions.

REFERENCES

1. **Amberg, S. M., A. Nestorowicz, D. W. McCourt, and C. M. Rice.** 1994. NS2B-3 proteinase-mediated processing in the yellow fever virus structural region: in vitro and in vivo studies. J. Virol. **68:**3794–3802.
2. **Arroyo, J., F. Guirakhoo, S. Fenner, Z. X. Zhang, T. P. Monath, and T. J. Chambers.** 2001. Molecular basis for attenuation of neurovirulence of a yellow fever virus/Japanese encephalitis virus chimera vaccine (ChimeriVax-JE). J. Virol. **75:**934–942.
3. **Bamford, J. K., D. H. Bamford, T. Li, and G. J. Thomas, Jr.** 1993. Structural studies of the enveloped dsRNA bacteriophage phi 6 of *Pseudomonas syringae* by Raman spectroscopy. II. Nucleocapsid structure and thermostability of the virion, nucleocapsid and polymerase complex. J. Mol. Biol. **230:**473–482.
4. **Burke, D. S., and T. P. Monath.** 2001. Flaviviruses, p. 1043–1125. *In* D. M. Knipe, P. M. Howley, et al. (ed.), Fields virology, 4th ed. Lippincott Williams & Wilkins, Philadelphia, Pa.

5. **Choi, H. K., G. Lu, S. Lee, G. Wengler, and M. G. Rossmann.** 1997. The structure of Semliki Forest virus core protein. Proteins Struct. Funct. Genet. **27:**345–359.
6. **Choi, H. K., L. Tong, W. Minor, P. Dumas, U. Boege, M. G. Rossmann, and G. Wengler.** 1991. Structure of Sindbis virus core protein reveals a chymotrypsin-like serine proteinase and the organization of the virion. Nature **354:**37–43.
7. **Ferlenghi, I., M. Clarke, T. Ruttan, S. L. Allison, J. Schalich, F. X. Heinz, S. C. Harrison, F. A. Rey, and S. D. Fuller.** 2001. Molecular organization of a recombinant subviral particle from tick-borne encephalitis virus. Mol. Cell **7:**593–602.
8. **Forsell, K., M. Suomalainen, and H. Garoff.** 1995. Structure-function relation of the NH_2-terminal domain of the Semliki Forest virus capsid protein. J. Virol. **69:**1556–1563.
9. **Harrison, S. C.** 2001. Principles of virus structure, p. 54–85. *In* D. M. Knipe, P. M. Howley, et al. (ed.), Fields virology, 4th ed. Lippincott Williams & Wilkins, Philadelphia, Pa.
10. **Heinz, F. X., and S. L. Allison.** 2001. The machinery for flavivirus fusion with host cell membranes. Curr. Opin. Microbiol. **4:**450–455.
11. **Heinz, F. X., S. L. Allison, K. Stiasny, J. Schalich, H. Holzmann, C. W. Mandl, and C. Kunz.** 1995. Recombinant and virion-derived soluble and particulate immunogens for vaccination against tick-borne encephalitis. Vaccine **13:**1636–1642.
12. **Heinz, F. X., K. Stiasny, G. Püschner-Auer, H. Holzmann, S. L. Allison, C. W. Mandl, and C. Kunz.** 1994. Structural changes and functional control of the tick-borne encephalitis virus glycoprotein E by the heteromeric association with protein prM. Virology **198:**109–117.
13. **Heinz, F. X., R. Berger, W. Tuma, and C. Kunz.** 1983. A topological and functional model of epitopes on the structural glycoprotein of tick-borne encephalitis virus defined by monoclonal antibodies. Virology **126:**525–537.
14. **Heinz, F. X., and C. Kunz.** 1981. Homogeneity of the structural glycoprotein from European isolates of tick-borne encephalitis virus: comparison with other flaviviruses. J. Gen. Virol. **57:**263–274.
15. **Heinz, F. X., W. Tuma, F. Guirakhoo, and C. Kunz.** 1986. A model study of the use of monoclonal antibodies in capture enzyme immunoassays for antigen quantification exploiting the epitope map of tick-borne encephalitis virus. J. Biol. Stand. **14:**133–141.
16. **Holzmann, H., K. Stiasny, M. Ecker, C. Kunz, and F. X. Heinz.** 1997. Characterization of monoclonal antibody-escape mutants of tick-borne encephalitis virus with reduced neuroinvasiveness in mice. J. Gen. Virol. **78:**31–37.
17. **Khromykh, A. A., and E. G. Westaway.** 1996. RNA binding properties of core protein of the flavivirus Kunjin. Arch. Virol. **141:**685–699.
18. **Khromykh, A. A., and E. G. Westaway.** 1997. Subgenomic replicons of the flavivirus Kunjin: construction and applications. J. Virol. **71:**1497–1505.
19. **Khromykh, A. A., H. Meka, K. J. Guyatt, and E. G. Westaway.** 2001. Essential role of cyclization sequences in flavivirus RNA replication. J. Virol. **75:**6719–6728.
20. **Kyte, J., and R. F. Doolittle.** 1982. A simple method for displaying the hydropathic character of a protein. J. Mol. Biol. **157:**105–132.
21. **Lanciotti, R. S., J. T. Roehrig, V. Deubel, J. Smith, M. Parker, K. Steele, B. Crise, K. E. Volpe, M. B. Crabtree, J. H. Scherret, R. A. Hall, J. S. MacKenzie, C. B. Cropp, B. Panigrahy, E. Ostlund, B. Schmitt, M. Malkinson, C. Banet, J. Weissman, N. Komar, H. M. Savage, W. Stone, T. McNamara, and D. J. Gubler.** 1999. Origin of the West Nile virus responsible for an outbreak of encephalitis in the northeastern United States. Science **286:**2333–2337.
22. **Lee, S., K. E. Owen, H. K. Choi, H. Lee, G. Lu, G. Wengler, D. T. Brown, M. G. Rossmann, and R. J. Kuhn.** 1996. Identification of a protein binding site on the surface of the alphavirus nucleocapsid and its implication in virus assembly. Structure **4:**531–541.
23. **Lescar, J., A. Roussel, M. W. Wien, J. Navaza, S. D. Fuller, G. Wengler, G. Wengler, and F. A. Rey.** 2001. The fusion glycoprotein shell of Semliki Forest virus: an icosahedral assembly primed for fusogenic activation at endosomal pH. Cell **105:**137–148.
24. **Lindenbach, B. D., and C. M. Rice.** 2001. Flaviviridae: the viruses and their replication, p. 991–1041. *In* D. M. Knipe, P. M. Howley, et al. (ed.), Fields virology, 4th ed. Lippincott Williams & Wilkins, Philadelphia, Pa.
25. **Lo, S. Y., M. J. Selby, and J. H. Ou.** 1996. Interaction between hepatitis C virus core protein and E1 envelope protein. J. Virol. **70:**5177–5182.
26. **Lobigs, M.** 1993. Flavivirus premembrane protein cleavage and spike heterodimer secretion require the function of the viral proteinase NS3. Proc. Natl. Acad. Sci. USA **90:**6218–6222.
27. **Lupas, A.** 1996. Coiled coils: new structures and new functions. Trends Biochem. Sci. **21:**375–382.
28. **Lupas, A.** 1997. Predicting coiled-coil regions in proteins. Curr. Opin. Struct. Biol. **7:**388–393.
29. **Mandl, C. W., S. L. Allison, H. Holzmann, T. Meixner, and F. X. Heinz.** 2000. Attenuation of tick-borne encephalitis virus by structure-based site-specific mutagenesis of a putative flavivirus receptor binding site. J. Virol. **74:**9601–9609.
30. **Mandl, C. W., M. Ecker, H. Holzmann, C. Kunz, and F. X. Heinz.** 1997. Infectious cDNA clones of tick-borne encephalitis virus European subtype prototypic strain Neudoerfl and high virulence strain Hypr. J. Gen. Virol. **78:**1049–1057.
31. **Mandl, C. W., F. X. Heinz, and C. Kunz.** 1988. Sequence of the structural proteins of tick-borne encephalitis virus (Western subtype) and comparative analysis with other flaviviruses. Virology **166:**197–205.
32. **Mandl, C. W., F. X. Heinz, E. Stockl, and C. Kunz.** 1989. Genome sequence of tick-borne encephalitis virus (Western subtype) and comparative analysis of nonstructural proteins with other flaviviruses. Virology **173:**291–301.
33. **Mandl, C. W., H. Holzmann, T. Meixner, S. Rauscher, P. F. Stadler, S. L. Allison, and F. X. Heinz.** 1998. Spontaneous and engineered deletions in the 3′ noncoding region of tick-borne encephalitis virus: construction of highly attenuated mutants of a flavivirus. J. Virol. **72:**2132–2140.
34. **Mandl, C. W., H. Kroschewski, S. L. Allison, R. M. Kofler, H. Holzmann, T. Meixner, and F. X. Heinz.** 2001. Adaptation of tick-borne encephalitis virus to BHK-21 cells results in the formation of multiple heparan sulfate binding sites in the envelope protein and attenuation in vivo. J. Virol. **75:**5627–5637.
35. **Markoff, L., B. Falgout, and A. Chang.** 1997. A conserved internal hydrophobic domain mediates the stable membrane integration of the dengue virus capsid protein. Virology **233:**105–117.
36. **McLauchlan, J.** 2000. Properties of the hepatitis C virus core protein: a structural protein that modulates cellular processes. J. Viral Hepat. **7:**2–14.
37. **McMinn, P. C.** 1997. The molecular basis of virulence of the encephalitogenic flaviviruses. J. Gen. Virol. **78:**2711–2722.
38. **Momany, C., L. C. Kovari, A. J. Prongay, W. Keller, R. K. Gitti, B. M. Lee, A. E. Gorbalenya, L. Tong, J. McClure, L. S. Ehrlich, M. F. Summers, C. Carter, and M. G. Rossmann.** 1996. Crystal structure of dimeric HIV-1 capsid protein. Nat. Struct. Biol. **3:**763–770.
39. **Owen, K. E., and R. J. Kuhn.** 1997. Alphavirus budding is dependent on the interaction between the nucleocapsid and hydrophobic amino acids on the cytoplasmic domain of the E2 envelope glycoprotein. Virology **230:**187–196.
40. **Perera, R., K. E. Owen, T. L. Tellinghuisen, A. E. Gorbalenya, and R. J. Kuhn.** 2001. Alphavirus nucleocapsid protein contains a putative coiled-coil alpha-helix important for core assembly. J. Virol. **75:**1–10.
41. **Reed, J. L., and H. Muench.** 1938. A simple method for estimating fifty percent endpoints. Am. J. Hyg. **27:**493.
42. **Rey, F. A., F. X. Heinz, C. W. Mandl, C. Kunz, and S. C. Harrison.** 1995. The envelope glycoprotein from tick-borne encephalitis virus at 2 Å resolution. Nature **375:**291–298.
43. **Ruggli, N., and C. M. Rice.** 1999. Functional cDNA clones of the Flaviviridae: strategies and applications. Adv. Virus Res. **53:**183–207.
44. **Russell, P. K., W. E. Brandt, and J. M. Dalrymple.** 1980. Chemikal and antigenic structure of flaviviruses, p. 503–529. *In* R. W. Schlesinger (ed.), The togaviruses: biology, structure, replication. Academic Press, New York, N.Y.
45. **Schalich, J., S. L. Allison, K. Stiasny, C. W. Mandl, C. Kunz, and F. X. Heinz.** 1996. Recombinant subviral particles from tick-borne encephalitis virus are fusogenic and provide a model system for studying flavivirus envelope glycoprotein functions. J. Virol. **70:**4549–4557.
46. **Skoging-Nyberg, U., and P. Liljeström.** 2000. A conserved leucine in the cytoplasmic domain of the Semliki Forest virus spike protein is important for budding. Arch. Virol. **145:**1225–1230.
47. **Skoging-Nyberg, U., and P. Liljeström.** 2001. M-X-I motif of Semliki Forest virus capsid protein affects nucleocapsid assembly. J. Virol. **75:**4625–4632.
48. **Skoging, U., M. Vihinen, L. Nilsson, and P. Liljeström.** 1996. Aromatic interactions define the binding of the alphavirus spike to its nucleocapsid. Structure **4:**519–529.
49. **Suomalainen, M., P. Liljeström, and H. Garoff.** 1992. Spike protein-nucleocapsid interactions drive the budding of alphaviruses. J. Virol. **66:**4737–4747.
50. **Wallner, G., C. W. Mandl, M. Ecker, H. Holzmann, K. Stiasny, C. Kunz, and F. X. Heinz.** 1996. Characterization and complete genome sequences of high- and low-virulence variants of tick-borne encephalitis virus. J. Gen. Virol. **77:**1035–1042.
51. **Wallner, G., C. W. Mandl, C. Kunz, and F. X. Heinz.** 1995. The flavivirus 3′-noncoding region: extensive size heterogeneity independent of evolutionary relationships among strains of tick-borne encephalitis virus. Virology **213:**169–178.
52. **Wynne, S. A., R. A. Crowther, and A. G. Leslie.** 1999. The crystal structure of the human hepatitis B virus capsid. Mol. Cell **3:**771–780.
53. **Yamshchikov, V. F., and R. W. Compans.** 1993. Regulation of the late events in flavivirus protein processing and maturation. Virology **192:**38–51.
54. **Zhao, H., B. Lindqvist, H. Garoff, C. H. von Bonsdorff, and P. Liljeström.** 1994. A tyrosine-based motif in the cytoplasmic domain of the alphavirus envelope protein is essential for budding. EMBO J. **13:**4204–4211.
55. **Zlotnick, A., S. J. Stahl, P. T. Wingfield, J. F. Conway, N. Cheng, and A. C. Steven.** 1998. Shared motifs of the capsid proteins of hepadnaviruses and retroviruses suggest a common evolutionary origin. FEBS Lett. **431:**301–304.